Pergamon

Int. J. Heat Mass Transfer. Vol. 38, No. 4, pp. 731–744, 1995

0017–9310/95 $9.50+0.00

0017–9310(94)E0111–7

Interaction of a dilute mist flow with a hot body

YU. A. BUYEVICH† and V. N. MANKEVICH

Department of Mathematical Physics, Urals State University, Ekaterinburg 620 083, Russia

(*Received* 26 *October* 1992)

Abstract—The flow of an aerosol containing liquid droplets around an overheated body is considered. The liquid mass flux is assumed small enough to prevent formation of a liquid film on the body surface. Depending on the relative normal velocity, impinging droplets are either captured by the surface and ultimately evaporated or almost elastically thrown away, this change in the droplet behaviour causing the onset of a heat transfer crisis. The theoretical description of the dynamic and thermal interaction between the droplets and the surface is reduced to solving two independent problems. The first problem consists in the analysis of the dynamic Leidenfrost phenomenon and further calculation of the critical normal velocity of a single droplet as a function of physical and process parameters. The second problem involves determination of the field of droplet trajectories around the body on the basis of the conventional theory of inertial capture of suspended particles and subsequent calculation of the total liquid mass flux onto the surface, conditioned by a requirement that the droplet fall velocity exceeds the indicated critical value. Both these problems are studied. The distributions of the specific coefficient of heat removal due to evaporation over the sphere, cylinder and plate surfaces in a uniform aerosol flow are obtained under different circumstances.

1. INTRODUCTION

Cooling of hot surfaces by a flow of air containing droplets of water or of another liquid is of great practical interest in many applications related to material processing. It offers a good opportunity to attain large local heat transfer coefficients as against those for a similar process of cooling by pure air under otherwise identical conditions. Sometimes, their values are comparable with those reached when using a pure liquid. At the same time, this can be readily achieved with a small expenditure, that is, without an excessive consumption of dispersed liquid. The abundance of such cooling processes in modern power engineering, metallurgy, cryogenics, and other fields of industry has necessitated the appearance of an enormous number of experimental works on the subject, representative examples of which are to be found in papers published over a period of several decades [1–8].

According to the majority of those works, the dependence of heat flux on the difference between the cooled wall temperature and the equilibrium boiling point of a dispersed liquid displays a descending segment, which bears a resemblance to that usually observed under the pool boiling conditions. Nevertheless, it appears to be due to quite different reasons in the case of a large liquid mass flux and a relatively small overheat compared with the opposite case of a small liquid flux and an appreciable overheat. In the first case a liquid film flowing along the wall is originated. Under steady external conditions, the film maintains a stationary state, since evaporation at the film free surface is completely compensated by an incessant liquid input coming from the collection of new droplets in the flow. Then the crisis seems to be merely a consequence of the transition from the bubbling to vapour-film heat transfer regime, just as happens in the pool-boiling processes.

Quite a different physical reason turns out to be responsible for the heat transfer crisis in the second case, where there is no film on the high-temperature wall. As a droplet approaches that wall, it experiences a repulsive force generated by an excessive pressure inside a thin intervening vapour layer which separates the droplet from the wall. The interlayer is produced by intensive evaporation at the flattened part of the droplet surface facing the wall. If the wall overheat is small, the approaching droplet is capable of making actual touching contact with the wall, in which case it spreads over and eventually evaporates on the wall, thereby contributing to the overall heat take-off. If the overheat exceeds a certain critical level dependent on the droplet size and velocity, on the wall temperature and the physical parameters, the droplet behaviour changes radically: the spreading out and subsequent evaporation give way to the elastic rebound of the droplet without a noticeable loss of liquid by evaporation. As a result, the wetting regime of dilute mist transfer is replaced by the non-wetting one. Such an effect of the change in the very nature of the dynamic and thermal interaction of an impinging droplet with an overheated surface must be justly related to the dynamic Leidenfrost phenomenon. The latter has been extensively investigated earlier for both solid [9, 10] and liquid [11, 12] hot surfaces.

† Present address: NASA Ames Research Center, Moffett Field, CA 94035, U.S.A.

NOMENCLATURE

a	vapour thermal diffusivity
E_1, E_2	constituents of droplet kinetic energy
f	total force acting on a droplet due to excessive pressure in vapour interlayer
G	function introduced in equation (17)
H	linear scale of immersed body
h	vapour interlayer thickness
I	dimensionless quantity introduced in equation (19)
J	liquid mass flux density
L	latent heat of evaporation
L_t, L_h	scales of time and length, respectively
l	thickness of liquid disc that models a droplet
n	number concentration of droplets in uniform flow
Q	total heat flux from hot body due to evaporation
q	heat flux density
q_1, q_2	heat absorbed by one droplet in wetting and non-wetting regimes, respectively
R	radius of liquid disc that models a droplet
R_0	droplet radius
St	Stokes number
T_L	dynamic Leidenfrost temperature
T_s	saturation (boiling) temperature of liquid
T_w	wall temperature
ΔT	overheat
Δt	droplet residence time
U	potential energy of surface tension, also velocity of uniform flow
u_*	critical droplet fall velocity
$\mathbf{V}$, $\mathbf{v}$	dimensionless and dimensional gas velocity
V	droplet volume
v_0	droplet fall velocity
We	Weber number
x	dimensionless radius of liquid disc
z_0	coordinate of liquid disc centre.

Greek symbols

α	attack angle
Δ	length scale of surface roughness
ε	dimensionless parameter defined in equation (16)
ζ, ξ	dimensionless variables of equations (15)–(17)
ζ_*	critical value of ζ determining capture cross section
η	dimensionless thickness of vapour interlayer
θ	angle coordinate
λ	vapour thermal conductivity
μ, ν	dynamic and kinematic vapour viscosity, respectively
ρ	liquid density
σ	surface-tension coefficient
τ, τ'	dimensionless times.

The mentioned situations of dense and dilute sprays are readily distinguishable in experiments since they display substantially different dependence on various physical and process parameters. For instance, dense spray film boiling is almost insensitive to the droplet size and is practically independent of the overheat, whereas in the dilute case both the droplet radius and wall overheat exhibit a drastic influence on heat removal from a cooled wall [7, 8]. This is quite conceivable, since in the first case the collection of droplets by the film depends on the droplet parameters merely through the droplet Stokes number influencing the process of inertial capture of droplets by a body immersed in a mist flow. Moreover, the temperature at the film–gas interface is the same irrespective of the actual cooled surface temperature, and as such does not affect the process altogether. Conversely, in the second case the process of the interaction of the surface with the impinging droplets is very sensitive to all the droplet parameters as well as to those that characterize the surface.

Theoretical investigation of the dispersed flow heat transfer is limited mostly to the film boiling regime with evaporation from the free film surface. Some examples of theoretical approaches suggested so far are given in refs. [13–15]. Attempts have also been made to retain the underlying concept of film boiling when dealing with the processes that involve rarefied mists in which nothing like a continuous film occurs [8]. This is obviously incorrect, and the study of such processes should be based, in fact, on the consideration of the behaviour of a single droplet normally falling onto a hot wall, as is the case in refs. [9, 10] and also in refs. [16, 17]. In the present paper only those processes are considered in which a cooled surface remains predominantly dry because the impinging droplets either rebound from the surface or have sufficient time to evaporate before a further portion of droplets will add liquid when hitting the surface in turn.

It should be emphasized that the paper has no relevance to the familiar problem of heat transfer of unidirectional dispersed flows in channels with high-temperature walls.

2. BASIC MODEL

When a cloud of droplets incident on a high-temperature body is sufficiently sparse, each droplet behaves almost like an independent object, save for the possible impact of a new droplet on the moist spot originated by the preceding one and for the possible effect of vapour emerging due to evaporation at the surface on other approaching droplets. It is evident that in the dilute limit the probability of the former event tends to zero and the influence of the latter effect has to degenerate. Thus, setting aside for the moment the discussion of collective effects of different origins, we shall resort to a tentative concept of independent droplets. Then, the total heat flux from the surface will consist of additive contributions from individual droplets except for a convective part resulting from heat transfer to the dispersed flow on the whole and for radiation.

Different constituents of the spray heat transfer as well as diverse observable behaviours of the droplets as they impact against the surface, such as rebound, disintegration and violent splashing, have been considered by many researchers and, in particular, in refs. [5, 8–11, 16]. As a first reliable approximation, such details may be ignored and it may be presented next that there is a sharp transition from the wetting regime of complete evaporation to the non-wetting rebound regime as the surface overheat grows. In the first regime the droplets spread out over the surface and add to the heat take-off by absorbing the latent heat needed to evaporate them. In the second regime the droplets are elastically repelled by the vapour cushion forming beneath them at the cooled surface, without an appreciable loss of mass. After that, they do not take part in heat transfer at all. With other conditions fixed, such a transition occurs at a certain definite value of the droplet fall velocity and apparently corresponds to the crisis commonly observed.

If one ignores heat transfer resulting from conduction, convection and radiation, then the onset of the crisis will signify the cessation of heat removal as the said value of the fall velocity is reached. That even such a rough picture is not so crude as it might appear is evidenced by numerous experiments. The excess of the total heat flux over that caused solely by the latent heat of the evaporation of liquid trapped by the surface constitutes not more than a few tens of per cent before the crisis and, similarly, just after the crisis that flux abruptly falls down to about twenty per cent or less of its original value [6]. Moreover, it means that the total flux in the evaporation regime may successfully be approximated by allowing only for the latent heat of the liquid–vapour phase transition.

The description of the dynamic interaction of individual droplets with a body immersed in a mist flow is always reduced to the study of the droplet trajectories which somewhat deviate from the flow streamlines due to inertial effects. If there were no repulsive forces, this purpose would have been accomplished by solving the familiar problem of the inertial capture of aerosol particles by a body [18–20]. According to the conventional theory of those phenomena, all the particles the trajectories of which intersect the body surface are supposed to be trapped if the secondary rebound is negligible. It means that any particle that actually touches the body is assumed to be retained by it.

If the body is overheated so that a vapour interlayer evolves bringing about the origination of a repulsive force which slows down the droplet under consideration as it undergoes deformation and flattens out while approaching the body, the field of droplet trajectories can be proved to remain the same as if the body were cold everywhere except for a narrow region in the close vicinity of the surface. Presuming the droplet Reynolds number to be large and neglecting the existence of that region, we are able to determine the trajectory field from a suitable solution of the inertial capture problem with no regard for the body overheat. In order to be actually caught by the surface, any droplet must have a normal velocity exceeding the above-mentioned critical value. It implies that only those droplets which satisfy the last requirement ought to be regarded as trapped and contributing to the heat removal, thus giving a necessary condition for finding out the liquid mass flux to the surface and then for evaluating the local heat transfer coefficient.

If the droplet fall velocity is maintained constant, the crisis can be described in an alternative way. As the temperature difference between the surface and the liquid on the verge of boiling increases, the total number of captured droplets firstly remains constant, then begins to decrease and finally comes to zero at a certain critical value of this difference. The corresponding surface temperature is commonly referred to as the dynamic Leidenfrost temperature.

Thus we arrive at two problems that have to be resolved when addressing the cooling of a hot body with the help of a dilute mist flow. First, the critical normal velocity must be found as a function of all the parameters at a given surface temperature. This amounts to developing the theory of the dynamic Leidenfrost phenomenon. Second, the field of droplet trajectories under appropriate flow conditions has to be determined, for which purpose it suffices to use the conventional theory of inertial capture. Such a subdivision of a rather complicated original problem into two simpler ones becomes possible since the details of the droplet interaction with the body surface are assumed to be of no consequence for the bulk of the flow. They are needed merely to decide whether a particular droplet will be captured or not.

The outline of the present paper is as follows. Firstly, the critical droplet impact velocity is found on the basis of the model developed in ref. [17]. This is done under the restriction that the initial droplet temperature coincides with that of boiling so that there is no need to consider the heating of droplets as they approach an overheated surface. This analysis leads to a very simple resulting expression of the critical velocity. Then, flows around a sphere and across a cylinder as well as around a plate at different attack angles are considered. This permits the effective cross section of inertial capture to be calculated as a function of that velocity and of other relevant parameters in all those cases. The findings allow the density distribution of the flux of captured droplets over the surface of a body of any indicated form as well as corresponding distribution of the local heat transfer coefficient due to evaporation to be obtained in different circumstances. The presentation partly follows that used by the present authors in their papers [17, 21], which seem to be hardly accessible to English-speaking readers.

It should be mentioned that the primary goal of the work is to give account of a concise and comprehensive physical picture of what happens when a thin mist flows across an overheated obstacle, rather than to work at particulars needed to correlate actual experiments.

3. DYNAMIC LEIDENFROST PHENOMENON

A rigorous analysis of the dynamic and thermal interaction of an overheated solid wall with an impinging droplet demands a joint problem of hydrodynamics and convective heat transport with an unknown interface to be studied with allowance for phase transition at the interface. This problem is overcomplicated and can hardly be resolved at present without resorting to a number of decisive simplifying assumptions. While referring the readers to ref. [17] for a thorough discussion of the problem, here the assumptions and main conclusions of the approximate model suggested in the paper cited will be briefly outlined.

First of all, the dependence of all the dynamic and thermophysical properties of both liquid and its vapour upon temperature are neglected. Furthermore, the following phenomena are purposely overlooked:

(1) viscous energy dissipation inside of a droplet which changes the droplet form as it approaches the wall;
(2) the reactive component of the total force acting on the droplet which is due to evaporation from the part of the interface facing the wall as well as the force constituents owing their origin to the gravity and fluid drag;
(3) the part of the excessive pressure within the vapour interlayer separating the droplet from the wall which is due to purely hydrodynamic factors originating when the interlayer gradually changes its thickness at a constant temperature and in the absence of evaporation;
(4) the forces of molecular attraction between the wall and the liquid–vapour interface; this might be of importance in the case of very smooth surfaces, but it can be shown to be negligible if the length scale of the wall roughness exceeds $\sim 10^{-7}$ m;
(5) dynamic and thermal slip effects which are also insignificant for rough surfaces.

In contrast to most of the works in which a great deal of attention has been paid to the above effects, it should be emphasized here that all of these effects can be proved to be of no major consequence for the process under study in the sense that they do not cause a considerable influence either quantitatively or quantitatively. (Exceptions are the effects (4) and (5) which are of crucial importance in the Leidenfrost phenomenon for both sessile and impinging drops in the case of a molecularly smooth wall [22].) Moreover, all of the above-enumerated assumptions can be avoided at the cost of making calculation more tedious and cumbersome but without introducing any major new difficulties.

Far more restrictive are additional assumptions which we put forward in order to get the necessary results in a tractable form. First, a liquid disc shown in Fig. 1(a) will be considered instead of the real deformable droplet. If the disc volume V is taken constant, then its radius R and thickness $2l$ are connected by the obvious relation

$$2\pi l R^2 = V = (4\pi/3)R_0^3. \tag{1}$$

Such an assumption is quite common in the current literature. In a general case, the arbitrary droplet form is described by using an infinite number of scalar parameters, such as coefficients, at different spherical harmonics needed for the purpose. The present assumption amounts, inasmuch as equation (1) holds true, to making use of only one scalar parameter (say, R) on purely empirical grounds, and so corresponds to the simplest way of defining the droplet form.

Second, the flow and heat transfer within the vapour interlayer of uniform thickness h are supposed to be quasi-stationary. This is permissible if the characteristic time scales, that is h^2/ν and h^2/a, are much smaller than the relevant time scale of the droplet motion near the wall, which is of the order of $h|\mathrm{d}h/\mathrm{d}t|^{-1}$.

Finally, to simplify the calculation, it is accepted that the impinging droplets are heated up to the equilibrium boiling temperature. This makes unnecessary the treatment of their heating in the vicinity of the wall. Generalization to the important case of subcooled droplets can be extended with the help of the methods developed in ref. [23].

Consider now the full energy of the droplet. It includes the kinetic energy E_1 of translational motion of the droplet as a whole, the kinetic energy E_2 of internal axisymmetric flow inside the droplet owing to the change in its form, and the potential energy U of surface tension [17]:

$$E_1 = \frac{\rho V}{2}\left(\frac{\mathrm{d}z_0}{\mathrm{d}t}\right)^2 \quad E_2 = \frac{\rho V}{2}\left(1+-\frac{8}{3}\frac{R_0^6}{R^6}\right)\left(\frac{\mathrm{d}R}{\mathrm{d}t}\right)^2$$

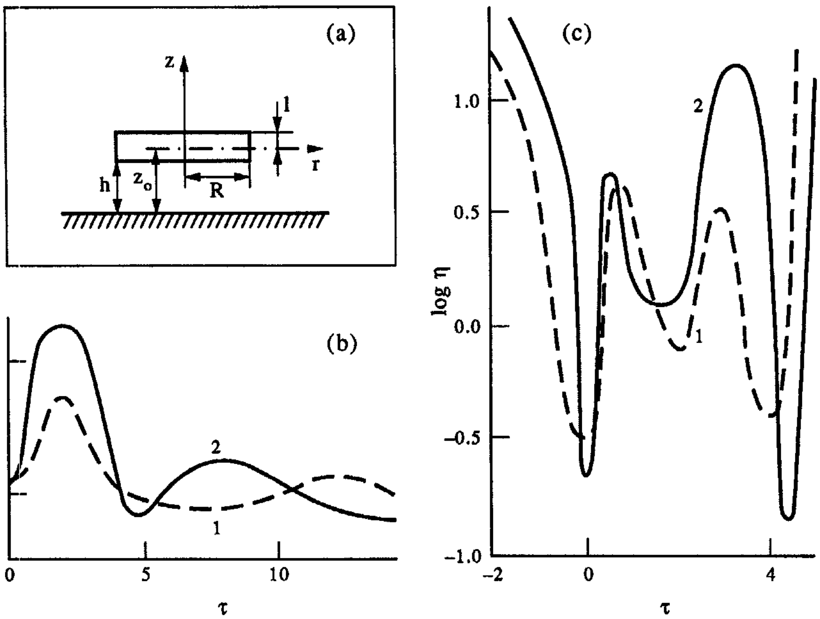

Fig. 1. Sketch of a droplet modelled as a liquid disc (a) and dynamics of a dimensionless disc radius (b) and vapour interlayer thickness (c) at $We = 1$ and 3 (dashed and solid curves, respectively).

$$U = 2\sigma\left(\pi R^2 + \frac{V}{R}\right) \tag{2}$$

where $z_0 = h+$, and V and l are related to R and R_0 by equation (1).

The energy conservation law yields

$$\mathrm{d}E_1 + \mathrm{d}E_2 + \mathrm{d}U = f\,\mathrm{d}h \tag{3}$$

where f is the force exerted by pressure on the droplet in the vapour interlayer. Complementary to equation (3) is the relation

$$\mathrm{d}E_1 = f\,\mathrm{d}z_0 = f(\mathrm{d}h + \mathrm{d}l) \tag{4}$$

which follows directly from Newton's second law.

To find the force f, we need to solve first the heat conduction problem under the conditions of constant temperatures T_w and T_s at the wall and interface, respectively, and then the hydrodynamic problem of flow within the planar vapour interlayer under the no-slip condition at the wall and with the vapour source at the interface. The source intensity is dictated by the requirement that all the heat transferred to the interface must be spent on evaporation. Neglecting radiation and omitting the intermediate calculations, we obtain the final result in the quasi-stationary approximation

$$f = \frac{3\pi}{2}\frac{\nu\lambda\Delta T}{L}\frac{R^4}{h^4} \quad \Delta T = T_w - T_s. \tag{5}$$

Let us introduce the following dimensionless variables and parameters:

$$x = \frac{R}{R_0} \quad \eta = \frac{h}{L_h} \quad \tau = \frac{t}{L_t} \quad We = \frac{\rho R_0 v_0^2}{6\sigma}$$

$$\varepsilon = \left(\frac{3}{4}\frac{\nu\lambda\Delta T}{\sigma L R_0}\right)^{1/4} \quad L_h = \left(\frac{3}{4}\frac{\nu\lambda\Delta T}{\sigma L}\right)^{1/4} R_0^{3/4}$$

$$= \varepsilon R_0 \quad L_t = \left(\frac{\rho R_0^3}{8\sigma}\right)^{1/2}. \tag{6}$$

Here L_h and L_t are the natural scaling parameters of length and time, respectively, We is the effective Weber number and ε presents a measure of the interlayer thickness in terms of the droplet size, and v_0 is the initial velocity of the droplet. The parameter ε for water, hydrocarbons and most other liquids is of the order of 10^{-2}–10^{-1} at $R_0 = 10^{-3}$ m. It becomes comparable with unity only for very small droplets which are molecular clusters rather than macroscopic objects. This means that ε can be used as a small parameter.

By using equations (1) and (2), equations (3) and (4) can be transformed into differential equations, which may be written down in an explicit dimensionless form with the help of equations (5) and (6). This yields [17]:

$$2\left(1 + \frac{8}{3x^6}\right)\frac{\mathrm{d}^2x}{\mathrm{d}\tau^2} - \frac{16}{x^7}\left(\frac{\mathrm{d}x}{\mathrm{d}\tau}\right)^2 + x - \frac{1}{x^2} = \frac{x}{\eta^4} \tag{7}$$

$$\frac{\mathrm{d}^2\eta}{\mathrm{d}\tau^2} - \frac{2}{x^3}\frac{\mathrm{d}^2x}{\mathrm{d}\tau^2} + \frac{6}{x^4}\left(\frac{\mathrm{d}x}{\mathrm{d}\tau}\right)^2 = \frac{1}{8}\frac{x^4}{\eta^4}.$$

The initial conditions, which correspond to the droplet falling from infinity onto the wall with an originally constant velocity v_0, are to be formulated in the following form:

$$x = 1 \quad \eta = \eta_0 > \frac{1}{\varepsilon}$$

$$\frac{dx}{d\tau} = 0 \quad \frac{d\eta}{d\tau} = -\frac{(We)^{1/2}}{\varepsilon} \quad \text{at } \tau = 0. \tag{8}$$

They agree with the substitution of the droplet by a disc and are convenient for numerical calculations.

Equations (7) govern a nonlinear oscillating system with two degrees of freedom. The amplitudes of the oscillations of dimensionless variables can be shown to be of the same order of magnitude, while the oscillation frequency scales with L_τ^{-1}. Typical dependences of x and η on dimensionless time are illustrated by Figs. 1(b) and (c). The initial period of aperiodic decrease in η and of corresponding increase in x reflects the approach of the droplet to the wall when the former gets considerably broadened and enlarges its surface, transforming the kinetic energy into the potential energy of surface tension. Next both x and η undergo irregular oscillations for some time, during which they reach several maxima and minima in succession. This is representative of the droplet bouncing on the underlying vapour cushion. After that, η soon becomes an infinitely increasing function, whereas both x and η continue to oscillate, the average of x tending to unity. This corresponds to the droplet rebound. That there is no damping of such residual oscillations is quite understandable, since within the framework of the above model no account is made of viscous dissipation. The asymptotic value of the droplet energy after the impact happens to be different from the initial energy because of the work accomplished by force f for the time of interaction with the wall through the vapour interlayer. The behaviour of the droplet, as revealed by solutions of equations (7) and (8), is consistent, with manifold phenomenological observations [9–12].

It should be pointed out that, within the framework of the model developed, the impinging droplet is surely repelled if the wall is smooth. This conclusion is entirely due to the neglect of the dependence of the boiling point on pressure in accordance with the liquid saturation line. Such a dependence is crucial for explaining the Leidenfrost phenomenon on molecularly smooth surfaces [22]. However, in practice it is insignificant for most real rough surfaces and so may be ignored.

Since the evolution of different quantities pertaining to the droplet behaviour has been discussed elsewhere [17], it will not be discussed here in more detail. What is important in the context of this paper is that the droplet will certainly be thrown away if the part of its surface facing the wall never contacts the projections on the wall in the course of the droplet bouncing. Thus, it is natural to accept that the crisis occurs when the smallest value of the interlayer thickness becomes equal to the mean height of the projections, which is characteristic of the wall roughness. This leads to a definition of the dynamic Leidenfrost temperature T_L through relations

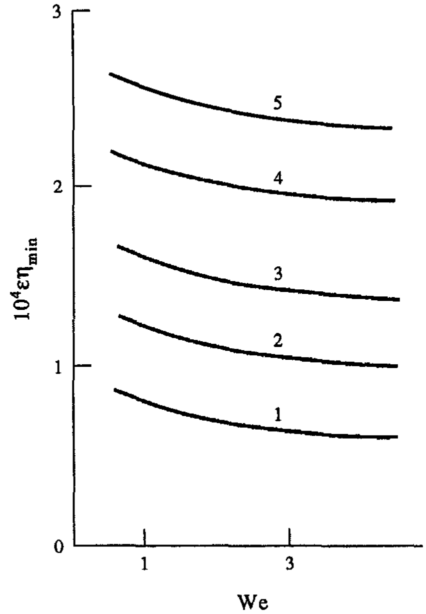

Fig. 2. Parameter $\varepsilon\eta_{min}$ vs We at $\varepsilon = 0.005, 0.01, 0.02, 0.05$ and 0.1 (curves 1–5, respectively).

$$T_L = T_s + \frac{4}{3}\frac{\sigma L R_0}{\nu\lambda}\varepsilon_L^4 \quad \varepsilon_L = \varepsilon\Big|_{T_w = T_L}$$

$$\Delta = L_h \eta_{min}(\varepsilon_L, We) = \varepsilon_L R_0 \eta_{min}(\varepsilon_L, We) \tag{9}$$

with the parameters ε and We being identified in equation (6). The quantity η_{min} as a function of those parameters has to be found by solving problems (7) and (8) with the help of numerical methods, as illustrated in Fig. 2.

Determination of either T_L with other parameters fixed or the critical value of We at a given T_w involves a tedious numerical calculation. To make the matter simpler, we turn our attention to elementary physical reasoning. It follows from the very form of equations (7) that η^4 can be excluded at negligible ε to yield the only equation for x which does not include η. This means that the droplet oscillations have to be approximately regarded as independent of the interlayer thickness. The inverse statement that the thickness should not depend on the droplet deformation at small ε has to be true as well. This amounts to a hypothesis that the functional dependence of η_{min} on ε and We incorporated into equations (9) must not contain any parameters affecting only the deformation, such as the surface-tension coefficient. There is a unique combination of ε and We that does not involve σ and, therefore, we get

$$\frac{\Delta}{R_0} = \varepsilon\eta_{min} = F\left(\frac{\varepsilon^4}{We}\right) \tag{10}$$

F being an unknown function of its argument.

A simple recalculation of the results shown in Fig. 2 gives the curves plotted in logarithmic coordinates

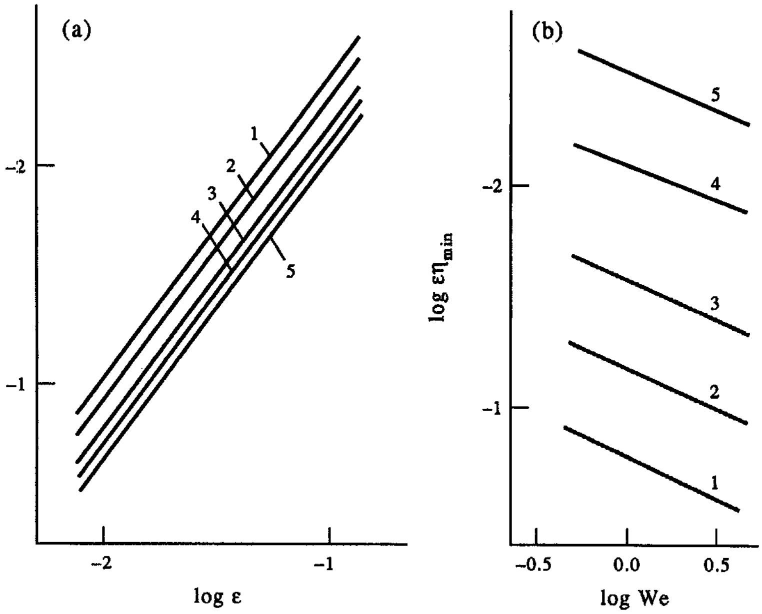

Fig. 3. Dependence of 10 g $\varepsilon\eta_{\min}$ on 10 g ε at $We = 0.5$, 1, 2, 3 and 5 (curves 1–5) (a) and on 10 g We at $\varepsilon = 0.005$, 0.01, 0.02, 0.05 and 0.1 (curves 1–5) (b).

in Fig. 3. The curves happen to be straight lines, and the analysis shows that $F(y) = Ay^{1/3}$, with A being an unknown numerical coefficient. Then equation (10) transforms into

$$\varepsilon We^{1/3}\,\eta_{\min} = A\varepsilon^{4/3}. \qquad (11)$$

To determine A, it is necessary to calculate the quantity on the left-hand side of equation (11) with the help of equations (7) subject to conditions (8). The results are collected in Table 1. The computations give $A = 0.7$. The use of the definitions in equations (6) and (11) yields

$$u_*^2 = \frac{3}{2}\frac{\nu\lambda R_0 \Delta T}{\rho L \Delta^3} \quad \Delta T = T_w - T_s. \qquad (12)$$

Thus, a lengthy and complicated manipulation leads to rather a simple representation of the desired critical fall velocity u_*. The non-wetting and wetting regimes of spray heat transfer occur when the normal component of the droplet velocity is smaller and larger than u_*, respectively. The dependence of the critical velocity on the droplet radius R_0 and wall overheat ΔT as well as on the physical parameters ν, λ and L is qualitatively confirmed by the bulk of available experiments. Of special interest is its strong dependence on the length scale Δ of wall roughness. Bearing in mind that the definition of Δ presents some difficulties, it is suggested that it should be regarded as an empirical parameter specific to the wall in question.

Table 1. Values of $10^4\varepsilon\, We^{1/3}\,\eta_{\min}$ at different We and ε

We	$We^{1/3}$	ε	$10^4\varepsilon\, We^{1/3}\,\eta_{\min}$
0.5	0.79	0.005	6.0
		0.01	15.0
		0.02	37.8
		0.05	128.1
		0.1	329.3
1.0	1.0	0.005	6.6
		0.01	18.4
		0.02	38.0
		0.05	128.8
		0.1	331.1
2.0	1.26	0.005	6.0
		0.01	15.1
		0.02	38.0
		0.05	128.8
		0.1	331.4
3.5	1.52	0.005	6.0
		0.01	15.2
		0.02	38.2
		0.05	129.4
		0.1	325.0
5.0	1.71	0.005	6.1
		0.01	15.2
		0.02	38.3
		0.05	129.7
		0.1	325.0

4. INERTIAL COLLECTION OF DROPLETS

Now we undertake a trajectory analysis of the capture of droplets from a uniform monodisperse gas–liquid mixture flow by immersed bluff solid obstacles. Because the gas density is much smaller than that of the liquid, it is possible to neglect all the gas inertial effects and write down an equation of Newton's second law for a single droplet in the following form [18, 19]:

$$St\frac{d^2\boldsymbol{\rho}}{d\tau'^2}+\frac{d\boldsymbol{\rho}}{d\tau'}=\mathbf{V}(\boldsymbol{\rho}) \qquad (13)$$

where the following new dimensionless variables and a parameter are introduced

$$\boldsymbol{\rho}=\frac{\mathbf{r}}{H}\quad \tau'=\frac{Ut}{H}\quad \mathbf{V}=\frac{\mathbf{v}}{U}\quad St=\frac{2\rho R_0^2 U}{9\mu H} \qquad (14)$$

r standing for the radius vector of the droplet centre and U and H being the gas velocity far upstream of an obstacle and the obstacle length scale, respectively. Initial conditions are to be imposed by requiring $d\mathbf{r}/dt$ to turn to U at an infinite distance from the obstacle. The mixture is assumed dilute, so that the gas velocity field $\mathbf{v}(\mathbf{r})$ is the same as in a similar pure gas flow and may be regarded as known. In what follows, the flow is considered as that of an ideal fluid with no account of the far-wake displacement effect or of the gas-phase flow separation, the influence of which was studied earlier in ref. [20].

4.1. *Collection efficiencies of cylindrical and spherical bodies*

A sketch of the flow either across a cylinder or around a sphere is given in Fig. 4(a). In the case of a cylinder equation (13) transforms into [21]

$$St\frac{d^2\xi}{d\tau'^2}+\frac{d\xi}{d\tau'}=1-\frac{\xi^2-\zeta^2}{(\xi^2+\zeta^2)^2}$$

$$St\frac{d^2\zeta}{d\tau'^2}+\frac{d\zeta}{d\tau'}=-\frac{2\xi\zeta}{(\xi^2+\zeta^2)^2} \qquad (15)$$

the definition of the dimensionless coordinates being evident from the sketch, and H being understood as the cylinder radius. This set of equations has to be integrated numerically to yield the droplet trajectory field. The dependence of the angular coordinate of the points of intersection of those trajectories with the cylinder surface at the droplet location far upstream at different Stokes numbers are presented in Fig. 4(b). The values $\zeta=\zeta_*(0)$ that correspond to $\theta=\pi/2$ determine the effective dimensionless cross section of the inertial collection of droplets $2\zeta_*$ under usual conditions, when it is sufficient for a droplet to touch the surface in order to be trapped.

However, if only those droplets make actual contact with the surface, the normal velocity of which is in excess of u_*, the collection efficiency is determined by the function $\zeta=\zeta_*(u_*/U)$. This quantity can be found by solving equations (15). Its dependence on u_*/U is plotted in Fig. 5. It is convenient to relate the number flux J of droplets to the upstream value $J_0=nU$ of this flux, n being the droplet number concentration. Then the solution of equations (15) enables us to draw the angular distribution of the dimensionless flux of the droplets that are really captured over the cylindrical surface. The corresponding curves are plotted in Fig. 6 at different values of St.

Similar results for a sphere are to be obtained in the same manner, save for the fact that equations (15) now have to be replaced by [21]

$$St\frac{d^2\zeta}{d\tau'^2}+\frac{d\xi}{d\tau'}=1-\frac{2\xi^2-\zeta^2}{2(\xi^2+\zeta^2)^{5/2}}$$

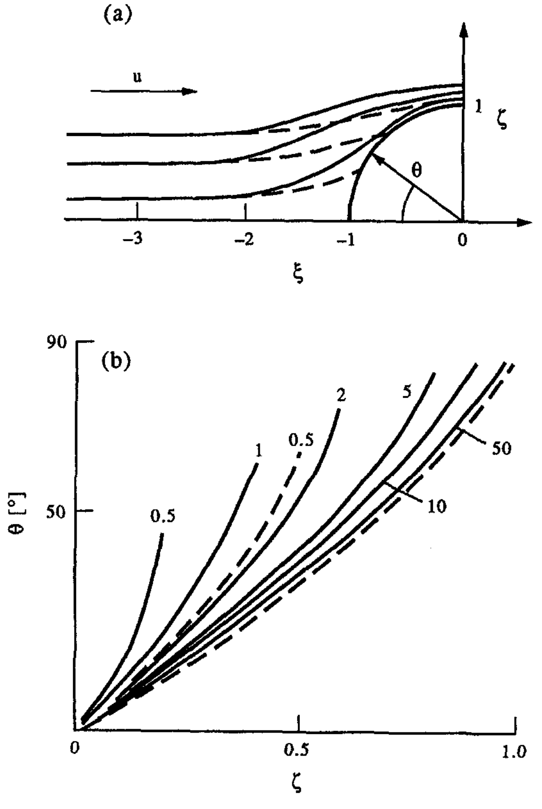

Fig. 4. Sketch of flow around a cylinder or sphere (a), solid and dashed curves represent streamlines and droplet trajectories, and dependence of the angular coordinate of the point of contact of a droplet with the surface on upstream droplet coordinate (b); solid and dashed lines in (b) pertain to a cylinder and sphere, respectively; figures at the curves give St values.

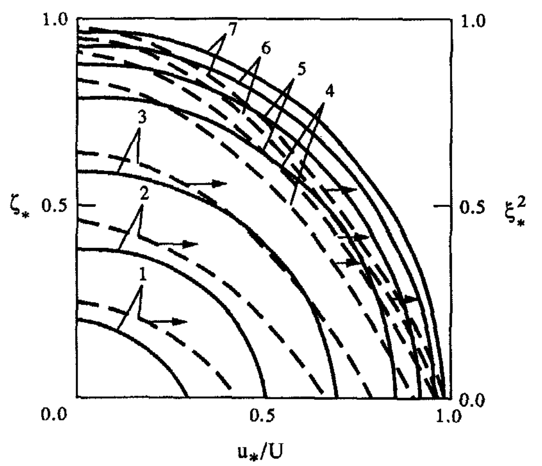

Fig. 5. Dimensionless effective droplet capture cross sections ζ_* (cylinder, solid lines) and ζ_*^2 (sphere, solid lines) vs u_*/U at $St=0.5$, 1, 2, 5, 10, 20 and 50 (curves 1–7, respectively).

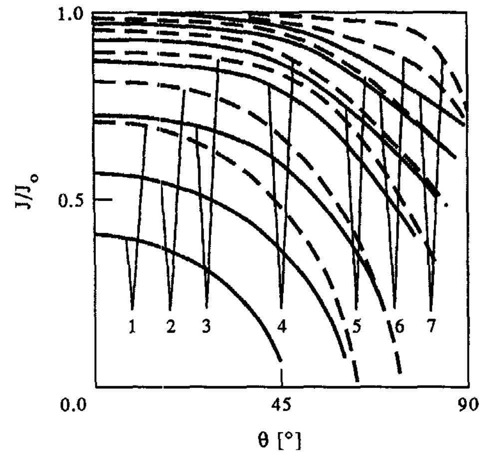

Fig. 6. Distribution of relative flux density of droplets over cylindrical and spherical surfaces; notation is the same as in Fig. 5.

$$St\frac{d^2\zeta}{d\tau'^2}+\frac{d\zeta}{d\tau'}=-\frac{3}{2}\frac{\xi\zeta}{2(\xi^2+\zeta^2)^{5/2}} \tag{16}$$

and that the capture cross section equals $\pi\zeta_*^2$. This is illustrated by dashed lines in Figs. 4(b), 5 and 6.

In both cases considered, ζ_* decreases monotonously as u_*/U grows. A maximum of ζ_* at $u_* = 0$ and a finite value of u_*/U at which ζ_* tends to zero are dependent only on the Stokes number. The droplets are collected by the central part of either the cylindrical or spherical surface with $\theta < \theta_*(u_*/U)$, θ_* turning to zero simultaneously with ζ_*.

4.2. *Collection efficiency of an inclined plate*

Flow across a solid plate of finite width is illustrated by Fig. 7. In this case equations (15) or (16) must be substituted by [21]

$$St\frac{d^2\xi}{d\tau'^2}+\frac{d\xi}{d\tau'}=G(\xi,\zeta)\sin\alpha$$

$$St\frac{d^2\zeta}{d\tau'^2}+\frac{d\zeta}{d\tau'}=\cos\alpha-G(\xi,\zeta)\sin\alpha$$

$$G(\xi,)=\left\{\frac{[(\xi^2+\zeta^2-1)^2+4\xi^2]^{1/2}-(\xi^2+\zeta^2-1)}{2[\xi^2+(\zeta+1)^2]}\right\}^{1/2}. \tag{17}$$

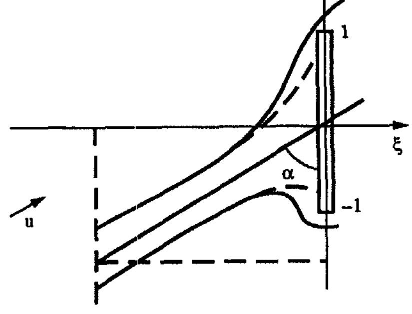

Fig. 7. Sketch of flow around a plate; solid and dashed curves show streamlines and trajectories of droplets.

Here the dimensionless variables explained in Fig. 7 are used and H is understood to be a half of the plate width. A model of flow without separation at the plate edges and with circulation, introduced to prevent the gas velocity from going to infinity at the back edge, is employed when writing down equations (17).

Figure 8 presents the distributions of the dimensionless normal velocity of droplets that come to the front part of the plate surface at different attack angles. As before, only those droplets whose normal velocity exceeds u_* are actually collected. A simple analysis of the curves in Fig. 8 evidences that this condition can be satisfied in the peripheral regions of the plate surface much easier than in the central region in the cases when the attack angle is either equal or is sufficiently close to $\pi/2$. If the flow is essentially oblique (small α), the droplets are mainly captured in the region adjacent to the front edge of the plate.

These results and the trajectory field, also to be found from solving equations (17), give an opportunity to deduce distributions of the droplet flux density over the plate surface similar to those drawn in Fig. 6. By way of example, such distributions at different values of St and α and at $u_* = 0$ are presented in Fig. 9.

4.3. *Heat transfer due to evaporation*

Droplets that are collected by the surface of an overheated body eventually evaporate and so provide for an effective heat removal. The heat flux density distribution caused by evaporation is governed by the corresponding droplet flux density J and is to be defined simply as

$$q = (4\pi/3)R_0^3\rho LJ. \tag{18}$$

The total amount of heat removed from the body as a result of droplet evaporation is to be found by integrating equation (18) over the whole body surface. The dependence of this quantity Q upon u_*/U at different values of St is illustrated for cylindrical and spherical bodies in Fig. 10, and also for plates at different values of St and α in Fig. 11. By using equation (12), one is able to recalculate the curves of Figs. 10 and 11 to get analogous dependences of Q on the body overheat $\Delta T = T_w - T_s$. As has already been pointed out, the constituent of the heat take-off due to evaporation can be thought of as a good approximation of the overall heat transfer from a body to a mist flow. This is why the mentioned curves as well as the dependences of Q upon ΔT may be interpreted as theoretical representatives of the declining sections of

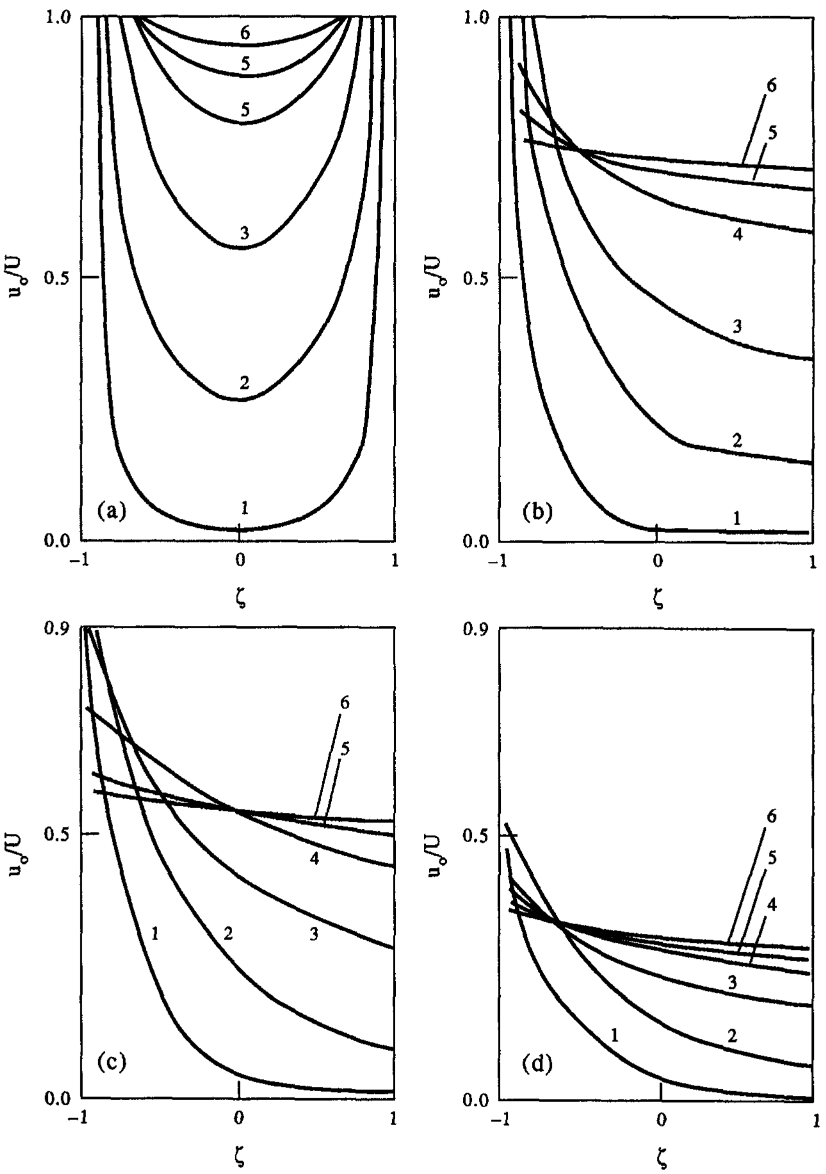

Fig. 8. Distribution of the dimensionless normal velocity of droplets making contact with the front part of the plate surface at various attack angles ((a), (b), (c) and (d) correspond to $\alpha = 90$, 45, 30 and 15°, respectively) and at $St = 0.5$, 1, 2, 5, 10 and 20 (curves 1–6, respectively).

the commonly observed mist flow heat transfer curves [1–8].

It should be stressed that, in compliance with the above discussion of collection efficiency and with the general character of those curves, the transition from the wetting to the non-wetting regime of heat transfer does not occur at some definite value of the body overheat but takes place gradually as the overheat increases within a certain range. Such an intermediate situation may be properly termed as a 'transition' heat transfer regime.

It is instructive to compare heat removal from a hot surface caused by the complete evaporation of the droplet with that ensured by the same droplet as it evaporates while bouncing on the vapour interlayer at the surface. In the first case the heat absorption is characterized by $q_1 = (4\pi/3)R_0^3\rho L$ (cf. equation (18)). In the second case

$$q_2 = \int_{-\infty}^{\infty} \pi R^2 \frac{\lambda \Delta T}{h} \mathrm{d}t = \pi R_0^2 \lambda \Delta T \frac{L_t}{L_h} I \quad I = \int_{-\infty}^{\infty} \frac{x^2}{\eta} \mathrm{d}\tau \tag{19}$$

where the scales L_t and L_h are identified in equation (6) and x and η have to be calculated with the help of the methods of the preceding Section. It is not difficult to show that the ratio q_2/q_1 is quite small under usual experimental and industrial conditions.

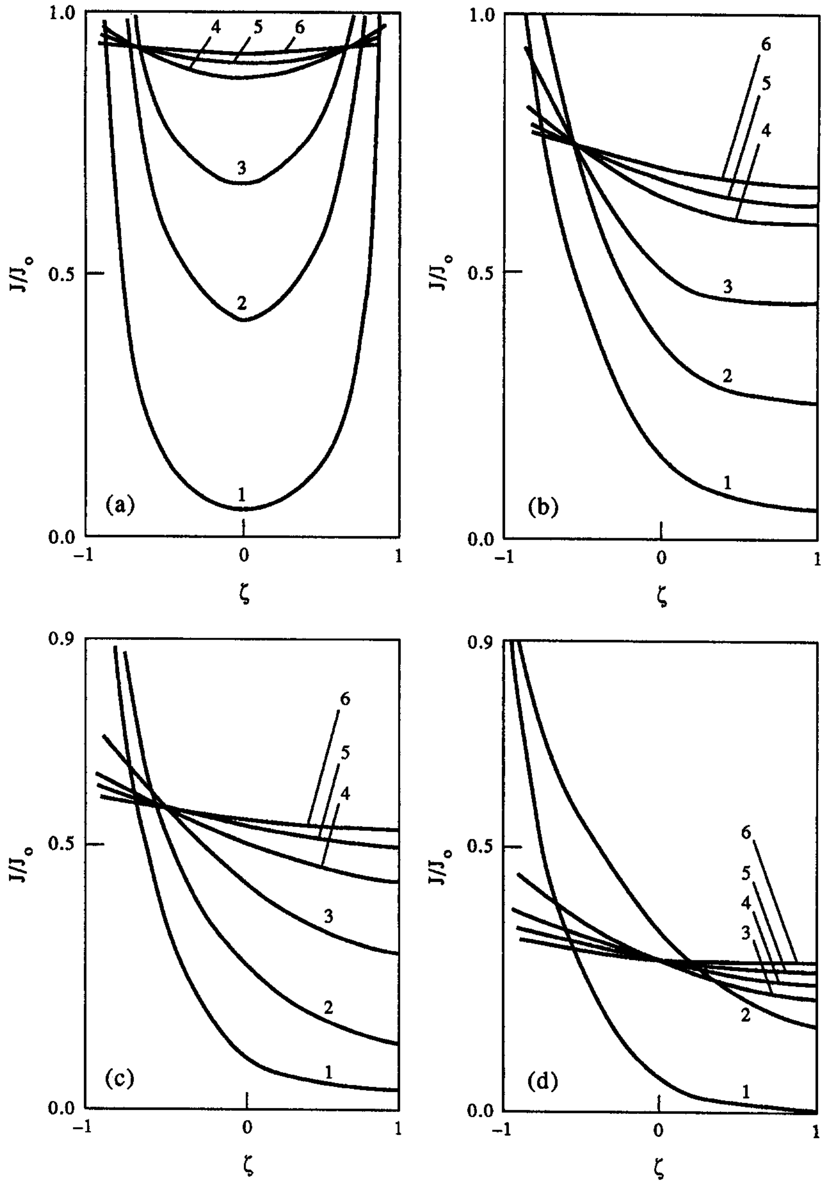

Fig. 9. Distribution of the relative droplet flux density over the front part of the plate surface; notation is the same as in Fig. 8.

A constituent of the overall heat transfer resulting from convective heat conduction can be described by standard means which are discussed in many textbooks and manuals, and so there is no need to dwell on them in this paper.

To conclude, it should be pointed out that application of the above methods is subject to the usual constraints of the conventional theory of aerosols. In particular, if droplets are very fine then inertial effects are negligible, and transport of the droplets to a surface is governed by either molecular or turbulent diffusion rather than by the processes of inertial collection [18, 19].

5. DISCUSSION

The novel feature of the developed theory is that it explains particulars of dilute mist flow heat transfer without introducing oversimplified empirical notions, in contrast to virtually all the previous relevant papers of which the present authors are aware. As a matter of fact, the contents of the present paper include two mutually supplemental sections. The first offers a realistic model of an elementary act of interaction of a single droplet with an overheated wall and so concerns modelling of the dynamic Leidenfrost phenomenon. The second section has relevance to the interaction of

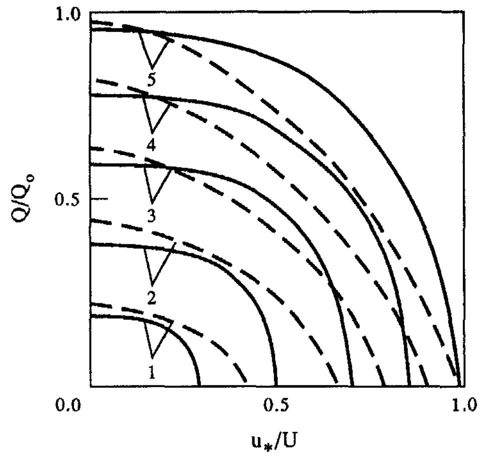

Fig. 10. Dimensionless total heat removal due to evaporation versus dimensionless critical velocity at $St = 0.5$, 1, 2, 5 and 50 (curves 1–5, respectively) from a cylinder and sphere (solid and dashed curves, respectively).

a flowing gas–liquid disperse mixture with a hot body under the assumption of mutual independence of the effects caused by individual droplets. Although a precise comparison of the obtained results with experimental findings is not part of the intended goal of this paper, the correlation of the model with accessible observations merits a brief discussion.

As pertains to the Leidenfrost phenomenon, a major difficulty is that different researchers use different sets of control parameters to correlate their results, hence a considerable scatter of data and some contradictions take place. With regard to this, it is worth noting that the paper could be helpful for experimentalists in that it indicates natural dimensionless parameters, namely *We* and ε, which should be used while evaluating and interpreting their findings. Nevertheless, there is a satisfactory agreement of the theory with experiments in both qualitative and quantitative respects, in spite of the approximate character of the theory.

By way of example, we consider the conclusions made in ref. [16]. In the non-wetting regime, the residence time Δt of a droplet on a heated wall can be defined, which has to be understood as the duration between the droplet impinging upon the wall and rebounding from it. It follows from Fig. 1, and from other calculations of the same kind, that the corresponding dimensionless time interval practically depends neither on *We* nor ε, and may be taken as $\Delta\tau = 6$. Then

$$\Delta t = L_t \Delta\tau = 0.75\left[\frac{\rho(2R_0)^3}{\sigma}\right]^{1/2}. \tag{20}$$

That this quantity is independent of the wall temperature is convincingly corroborated by ref. [16]. Moreover, the numerical coefficient 0.75 that appears in equation (20) is close to $\pi/4 = 0.785$. The latter value results from relating Δt to the natural vibration frequency of a liquid sphere and provides for a good quantitative agreement with the experimental data [16].

Furthermore, by using equations (9) and (11), one gets the following formula for the dynamic Leidenfrost temperature

$$T_L = T_s + 0.65\frac{\rho L}{\nu\lambda}\frac{v_0^2\Delta^3}{R_0}. \tag{21}$$

The dependence of T_L on R_0 was measured in ref. [16] as well. However, the relationship between v_0 and R_0 remained unknown. Although the droplet fall velocity v_0 could vary somewhat at fixed radius, there is a strong correlation between these two variables. The correlation can approximately be described with the help of the quadratic fluid drag law for steady fall of a droplet under gravity, which gives $v_0 \sim R_0^{1/2}$. Then T_L in equation (21) happens to be insensitive to the

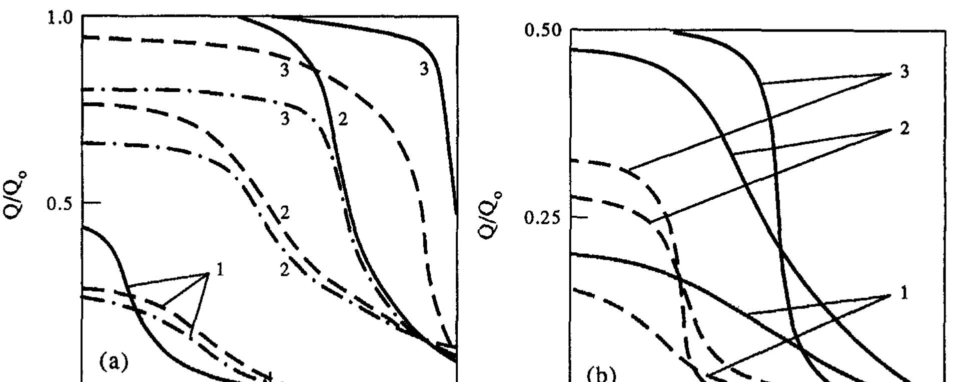

Fig. 11. Dimensionless total heat removal due evaporation from a plate as a function of dimensionless critical droplet velocity at $\alpha = 90$, 60 and 45° (in (a) solid, dashed and chain-dotted lines, respectively) and at $\alpha = 30$ and 15° (solid and dashed curves in (b)): curves 1–3 correspond to $St = 0.5$, 2 and 10, respectively.

droplet size, as was concluded in ref. [16]. Moreover, there is a good quantitative agreement between equation (21) and the data for water and ethanol droplets [16].

When turning to heat removal from the wall ensured by a single droplet in the non-wetting regime, we must use equation (19) which can be rewritten in the form

$$q_2 = C\left(\frac{\rho^2 L}{\sigma v}\right)^{1/4} (\lambda \Delta T)^{3/4} R_0^{11/4} I \qquad (22)$$

C being a numerical coefficient.

Evaluations of I based on the definition of I in equation (19) show it as being weakly dependent on We, if We is not too small. Next, the characteristic values of dimensionless variables η and x during the period of the droplet bouncing at the wall are directly and inversely proportional to ε, respectively, within the finite ranges of the latter parameter. This makes for a rough estimate $I \sim \varepsilon^{-3}$, so that equation (22), with allowance for equation (6), yields

$$q_2 \sim (L/v)\,(\rho\sigma)^{1/2} R_0^{7/2}. \qquad (23)$$

However crude, this estimate evidences that q_2 ought to be almost independent of the overheat and the fall velocity at fixed R_0, which again agrees with the observations of ref. [16]. That both the wall overheat and the droplet velocity have little effect upon heat transfer in the non-wetting regime complies with observations of others (e.g. refs. [9–12]). The dependence of q_2 on the droplet size deviates somewhat from that in ref. [16] where it was concluded that the heat absorption attributed to one droplet should increase with the droplet diameter cubed. Nonetheless, the difference is not large.

In the dilute limit, the distribution of the heat flux density due to evaporation over the cooled surface is to be obtained by multiplying either q_1 or q_2 by J (cf. equation (18)). Since the droplet parameters influence the collection efficiency and so affect the liquid mass flux density J, the dependence of the heat flux density on these parameters is modified as compared with that of heat absorption per droplet. However, the dependence on the overheat remains the same. These conclusions hold for both wetting and non-wetting regimes and agree with experimental evidence. However, the situation changes in the transition regime.

Inherent to the last regime is that the surface under question is divided into two regions, in which the non-wetting and wetting regimes are established. As the surface overheat grows at all other parameters fixed, the former region expands and the latter one contracts and then vanishes. Thus the overall heat flux becomes dependent on the parameters in a more complicated way and, in particular, decreases monotonously with the overheat. This is consistent with all the known observations and explains the crisis of dilute mist heat transfer. Direct comparison of theoretical predictions with experiments is hindered by the latter usually being carried out under flow conditions essentially different from those considered above (for instance, under jet flow conditions). Nevertheless, the distribution of the liquid mass flux over a cylindrical surface (Fig. 6) is well confirmed by the results of ref. [20].

It is not intended to indicate here the possible ways of avoiding the restrictive assumptions imposed earlier, especially as such ways are for the most part quite obvious. Three promising directions of future work should be mentioned. First, to study the effect of subcooling of impinging droplets, it is necessary to consider the heating of a droplet as it approaches a hot wall, for which purpose the methods suggested in ref. [23] are applicable. Second, it seems to be reasonable to treat a local drop in the wall temperature beneath an evaporating droplet, for which purpose a combined problem of heat conduction in both the vapour interlayer and the bulk of a cooled body has to be investigated. Thirdly, even though collisions of droplets near the body surface might be ignored, the evaporation gives rise to a vapour flow off the surface that can effect the behaviour of the impinging droplets to a considerable extent and, moreover, can cause the occurrence of a peculiar self-oscillating regime of dilute mist heat transfer [24].

REFERENCES

1. R. Z. Alimov, Heat transfer in two-phase flow across a heated cylindrical tube, *Zh. Tekh. Fiz.* **26,** 1292–1305 (1956).
2. H. Junk, Wärmeübergangsuntersuchungen an einer simulierten Secundärkühlstrecke für das Strangiessen von Stahl, *Neue Hütte* H **1,** 13–18 (1972).
3. C. J. Hoogendorn and R. den Hond, Leidenfrost temperature and heat transfer coefficients for water sprays impinging on a hot surface, *Proceedings 5th Transfer Conference*, Vol. 4, pp. 135–138, Tokyo (1974).
4. P. G. Kosky, Heat transfer to saturated mist flowing normally to a heated cylinder, *Int. J. Heat Mass Transfer* **19,** 539–543 (1976).
5. E. N. Ganic and W. M. Rohsenow, Dispersed flow heat transfer, *Int. J. Heat Mass Transfer* **20,** 855–866 (1977).
6. W. M. Rohsenow, Needed research in boiling heat transfer. In *Heat Transfer in Energy Problems*, pp. 51–58. Hemisphere, Washington, DC (1983).
7. K. J. Choi and S. C. Yao, Mechanisms of film boiling heat transfer of normally impacting spray, *Int. J. Heat Mass Transfer* **30,** 311–318 (1987).
8. S. Deb and S. C. Yao, Analysis of film boiling heat transfer of impacting sprays, *Int. J. Heat Mass Transfer* **32,** 2099–2112 (1989).
9. L. H. J. Wachters and W. A. J. Westerling, The heat transfer from a hot wall to impinging drops in the spheroidal state, *Chem. Engng Sci.* **21,** 1047–1056 (1966).
10. C. O. Pedersen, An experimental study of the dynamic behaviour and heat transfer characteristics of water droplets impinging upon a heated surface, *Int. J. Heat Mass Transfer* **13,** 369–381 (1970).
11. K. L. Waldram, H. K. Fauske and S. G. Bankoff, Impaction of volatile liquid droplets onto a hot liquid surface, *Can. J. Chem. Engng* **54,** 456–458 (1976).
12. Y. Iida and T. Takashima, Direct-contact heat transfer characteristics: evaporation of a drop dropped onto a

hot liquid surface, *Int. J. Heat Mass Transfer* **23,** 1263–1271 (1980).
13. J. W. Hodgson and J. E. Sunderland, Heat transfer from a spray-cooled isothermal cylinder, *Ind. Engng Chem. Fund.* **7,** 567–572 (1968).
14. I. C. Finlay, An analysis of heat transfer during flow of an air–water mist across a heated cylinder, *Can. J. Chem. Engng* **49,** 333–339 (1971).
15. W. S. Fu and G. C. Yang, Influence of droplets' trajectories and size distribution on heat transfer from a wedge in an air–water mist flow, *Numerical Heat Transfer* **16A,** 155–174 (1989).
16. M. Shoji, T. Wakunaga and K. Kodama, Heat transfer from a heated surface to an impinging subcooled droplet, *Trans. Japan Soc. Mech. Engrs* **50,** 716–722 (1984).
17. Yu. A. Buyevich, V. N. Mankevich and M. I. Polotsky, Toward the theory of fall of a droplet onto an overheated surface, *Teplofiz. Vysok. Temp.* **24,** 743–752 (1986).
18. N. A. Fuchs, *Mechanics of Aerosols.* Pergamon, New York (1964).
19. V. M. Voloshchuk, *Introduction to Mechanics of Coarsely Dispersed Aerosols.* Gidrometeoizdat, Leningrad (1971).
20. T. Aihara and W. S. Fu, Effects of droplet-size distribution and gas-phase flow separation upon inertia collection of droplets by bluff bodies in gas–liquid mist flow, *Int. J. Multiphase Flow* **12,** 389–403 (1986).
21. K. N. Agafonov, Yu. A. Buyevich and V. N. Mankevich, Toward the theory of cooling of surfaces with flows of dropwise aerosols, *Teplofiz. Vysok. Temp.* **29,** 115–120 (1991).
22. Yu. A. Buyevich and V. N. Mankevich, Toward the theory of evaporation of liquid in the spheroidal state, *Doklady AN SSSR* **262,** 1373–1377 (1982).
23. V. N. Mankevich and K. N. Agafonov, On the dynamic Leidenfrost temperature for subcooled drops, *J. Engng Phys.* **58,** 645–650 (1990).
24. M. A. Brich, Interaction of flow of a dispersed liquid with a heated surface, *J. Engng Phys.* **40,** 35–40 (1981).